Journal of Hydrology 559 (2018) 71–83

Contents lists available at ScienceDirect

Journal of Hydrology

journal homepage: www.elsevier.com/locate/jhydrol

Research papers

# Spatial and temporal evapotranspiration trends after wildfire in semi-arid landscapes

Patrick K. Poon, Alicia M. Kinoshita *

*San Diego State University, 5500 Campanile Drive, San Diego, CA, USA*

ARTICLE INFO

*Article history:*
Received 10 August 2017
Received in revised form 7 February 2018
Accepted 11 February 2018
Available online 13 February 2018
This manuscript was handled by T. McVicar, Editor-in-Chief, with the assistance of Patrick N. Lane, Associate Editor

*Keywords:*
Evapotranspiration
Wildfire
Remote sensing
Disturbance hydrology

ABSTRACT

In recent years climate change and other anthropogenic factors have contributed to increased wildfire frequency and size in western United States forests. This research focuses on the evaluation of spatial and temporal changes in evapotranspiration (ET) following the 2011 Las Conchas Fire in New Mexico (USA) using the Operational Simplified Surface Energy Balance Model (SSEBop ET). Evapotranspiration is coupled with soil burn severity and analyzed for 16 watersheds for water years 2001–2014. An average annual decrease of 120 mm of ET is observed within the regions affected by the Las Conchas Fire, and conifers were converted to grassland a year after the fire. On average, the post-fire annual ET in high, moderate, and low burn severity is lower than pre-fire ET by approximately 103–352 mm, 97–304 mm, and 91–268 mm, respectively. The ratio of post-fire evapotranspiration to precipitation (ET/P) is statistically different from pre-fire conditions ($\alpha = 0.05$) in nine of the watersheds. The largest decrease in ET is approximately 13–57 mm per month and is most prominent during the summer (April to September). The observed decrease in ET contributes to our understanding of changes in water yield following wildfires, which is of interest for accurately modeling and predicting hydrologic processes in semi-arid landscapes.

© 2018 Elsevier B.V. All rights reserved.

## 1. Introduction

Forests cover approximately 42 million km$^2$ (or 30% of the land surface) in tropical, temperate, and boreal lands (Bonan, 2008) and are critical regulators in the terrestrial water balance through evapotranspiration (ET). Evapotranspiration is an energy-water flux that redistributes water from the soil and plant surfaces (evaporation) and vegetation (transpiration) into the atmosphere (Allen et al., 2005) and is sensitive to vegetation characteristics and climate. In temperate eucalypt forests and semiarid forests, annual ET accounts for 70–80% and 85–100% of precipitation, respectively (Vertessy et al., 2001; Yaseef et al., 2010; Mitchell et al., 2012). While in loblolly pine (*Pinus* taeda) plantations in the southeastern U.S. and ponderosa pine (*Pinus ponderosa*), approximately 70% (Sun et al., 2002) and 85%, respectively, of annual precipitation contributes to ET (Montes-Helu et al., 2009). Evapotranspiration influences climate through energy and water exchange, making forests essential for ecological and watershed services such as flood control, water quality, and carbon and nitrogen storage.

Disturbances in forests, such as wildfires, floods, landslides, and clearcutting can promote healthy tree density, herbaceous and shrub production, water availability and runoff, nutrient availability, soil characteristics, and wildlife habitat (Covington and Moore, 1994). However, global climate changes, largely due to anthropogenic activities, have led to variations in temperature and precipitation regimes, altering natural wildfire patterns, drought, and other forest disturbances (Dale et al., 2001). In the western U.S., climate change contributes to longer dry summer seasons and drier vegetation, and extended wildfire durations and seasons, which subsequently leads to more frequent and intense wildfires. (Dale et al., 2001; Westerling et al., 2006). Invasive species can also impact ecosystem processes and change vegetation composition, which impacts fuel properties and fire regimes such as intensity, frequency, and seasonality of wildfires (Brooks et al., 2004). Following wildfires, lower ET is expected from the loss of foliar volumes and transpiration processes. Also, the replacement of deep-rooted high profile trees by low profile grasses may contribute to lower ET (Neary et al., 2005). The reduced ET means less precipitation is converted into vapor, and thus more water generally is available for streamflow. Given the large role of ET in the water budget, a disturbance can shift the partitioning between dominant water fluxes such as infiltration and surface runoff. Thus, accurate estimates of

* Corresponding author.
*E-mail addresses:* ppoon@sdsu.edu (P.K. Poon), akinoshita@mail.sdsu.edu (A.M. Kinoshita).

https://doi.org/10.1016/j.jhydrol.2018.02.023
0022-1694/© 2018 Elsevier B.V. All rights reserved.

ET are necessary for climate studies, ecosystem modeling, and agriculture and hydrologic applications, especially in regions experiencing acute or chronic changes in land cover.

Post-fire watershed processes in various ecosystems have been documented, including altered sediment yield (Keller et al., 1997; Lane et al., 2006), soil moisture (Ebel, 2013), peak streamflow (Veenhuis, 2000), base flow (Kinoshita and Hogue, 2011), snow accumulation and melt patterns (Neary et al., 2005; Micheletty et al., 2014) and surface water yield (Kinoshita and Hogue, 2015). Bart (2016) noted a 134% increase of streamflow during the first year after fire in 12 watersheds in southern California. Similarly, Kinoshita and Hogue (2015) observed an increase in low streamflow volume (118%–1090%) following the 2003 Old Fire in southern California. The enhanced baseflow in the chaparral dominated watersheds was attributed to the reduction of basin-wide transpiration rates due to the loss of vegetation (Kinoshita and Hogue 2011; 2015). In New Mexico, Wine and Cadol (2016) observed various post-fire streamflow responses in three semi-arid watersheds that were impacted by monsoon storms from 1982 to 2014. The runoff in the Gila watershed (92% burned) was 12–16 times greater than unburned watersheds for 3–5 post-fire years (Wine and Cadol, 2016). The reduced transpiration and increased infiltration-excess overland flow following monsoon storms contributed to increased streamflow. Some watersheds did not show an increased post-fire water yield, which was attributed to the inaccuracy of runoff measurements, increased transpiration by remaining plants, and increased evaporation as a result of reduced tree canopy (Wine and Cadol, 2016). Similarly, Feikema et al. (2013) did not observe an increase of initial post-fire streamflow due to reduced canopy cover, which highlights the importance of antecedent soil moisture conditions. During a drought, low rainfall can result in soil water deficits. For example, when soil moisture deficits are very large or very small (Feikema et al., 2013; Bart, 2016), surface runoff may not be impacted by changes in evapotranspiration. Benavides-Solorio and MacDonald (2001) noted that low runoff may be due to high antecedent soil moisture or dry soils, with a higher capacity for infiltration, even in high burn severity regions. Based on the limited literature, Wine and Cadol (2016) noted the importance of continuing research on the impacts of wildfire on evapotranspiration to further understand post-fire hydrologic and vegetation processes and improve the prediction of streamflow responses.

There is limited research focused on post-wildfire ET. Post-fire ET studies by Montes-Helu et al. (2009) and Dore et al. (2010) observed $CO_2$ and ET using eddy covariance data applicable for an area of 176 (±3) m (burned) and 271 (±4) m (unburned) during 2006 in Arizona after a severe fire in 1996. After the fire, the ponderosa pine became primarily grassland and shrub with 40% vegetation coverage, 50% bare soil, and 10% logs and snags (Montes-Helu et al., 2009). Dore et al. (2010) noted that post-fire ET was lower for 10–11 years after the fire by 76–116 mm per year. Another field-based study in a mixed eucalypt forest located in the state of Victoria, Australia, observed that ET in high and moderately burned forest are 41% and 3% lower, respectively, over the first two post-fire years (Nolan et al., 2014). Utilizing remote sensing techniques, Sánchez et al. (2015) applied a two-source energy balance approach on two sets (6–7 years and 11 years after the fire) of satellite-based scenes (a total of 15 Landsat 5 Thematic Mapper and Enhanced Thematic Mapper Plus images) to estimate latent heat flux (heat associated with surface evaporation) after a wildfire in Spain. Sánchez et al. (2015) noted a decrease of approximately 1 mm per day of ET in unburned pine forest, 6–7 years after fire. This decrease was attributed to altered vegetation structure, land surface temperature, and albedo (Sánchez et al., 2015). Dore et al. (2010) and Nolan et al. (2014) provided important insight into point-scale evaporative processes after wildfire, while Sánchez et al. (2015) provided a higher spatial resolution study with limited temporal resolution.

This research builds upon previous studies by incorporating remote sensing products to quantify post-fire evapotranspiration at higher temporal and spatial scales. Evapotranspiration before and after the 2011 Las Conchas Fire in New Mexico, United States was investigated utilizing the Operational Simplified Surface Energy Balance Model (SSEBop). Pre- and post-fire ET patterns were compared with spatially distributed precipitation and soil burn severity for water years (WY) 2001 to 2014 (October 1, 2000 to September 31, 2014). This research addresses the following questions, which also provides the structural sub-headings used in the following Methods, Results, and Discussions sections:

I. How well does SSEBop ET represent pre- and post- fire processes?
II. How does annual and seasonal ET change after wildfire?
III. How does pre- and post- fire ET vary spatially and temporally with respect to soil burn severity?

## 2. Data and study site

### 2.1. Spatial actual evapotranspiration model

Single source energy balance models such as the Surface Energy Balance Algorithm for Land (SEBAL; Bastiaanssen et al., 1998) and Mapping Evapotranspiration at high Resolution with Internalized Calibration (METRIC; Allen et al., 2007) require manually selected hot and cold reference pixels to compare climatic conditions for one satellite image. The Simplified Surface Energy Balance Index (SSEB-I) and Operational Simplified Surface Energy Balance Model (SSEBop; Senay et al., 2013) omit the calculation of sensible heat flux to reduce the complexity of determining actual ET. SSEBop also assumes that each pixel has pre-defined hot and cold reference values, given that reference points are stationary or the differences are small in relation to the accuracy level obtained through varying boundary conditions (Senay et al., 2013). This approach requires a pre-defined satellite-derived temperature difference (dT), which is based on net radiation, air resistance, Normalized Difference Vegetation Index (NDVI), and air temperature (2–4) (Senay et al., 2013). The ET fraction (ETF) is calculated from hot, cold, and observed surface temperatures (5). Finally, SSEBop actual ET ($ET_a$) is estimated by multiplying the Penman-Montieth reference ET ($ET_o$ (1)) and the ETF (6). The Penman-Montieth (Monteith, 1965) equation is expressed as:

$$ET_o(\text{mm/day}) = \frac{\Delta(R_n - G) + \left[\rho_a C_p \frac{(e_s - e_a)}{r_a}\right]}{\Delta + \gamma\left(1 + \frac{r_s}{r_a}\right)} \quad (1)$$

where $R_n$ = clear sky net radiation (W $m^{-2}$); G = soil heat flux (W $m^{-2}$); $(e_s - e_a)$ = the vapor pressure deficit of the air (Pa); $\rho_a$ = mean air density (kg $m^{-3}$); $c_p$ = specific heat of the air (J $kg^{-1}$ $K^{-1}$); = slope of the saturation vapor pressure temperature relationship (Pa $K^{-1}$), $\gamma$ = psychrometric constant (~66 Pa $K^{-1}$), $r_s$ and $r_a$ are the (bulk) surface and aerodynamic resistances (s $m^{-1}$). The SSEBop ET algorithm consists of (Senay et al., 2013):

$$T_h = T_c + dT \quad (2)$$

$$dT = \frac{R_n \times r_{ah}}{\rho_a \times C_p} \quad (3)$$

$$T_c = T_h \times c \quad (4)$$

$$ETF = \frac{T_h - T_s}{T_h - T_c} \quad (5)$$

$$ET_a = ET_o \times ETF \times k \quad (6)$$

where $T_h$ = Temperature of "hot" condition (K); $T_c$ = Temperature of "cold" condition (K); $T_s$ = Land Surface Temperature (K); $r_{ah}$ = aerodynamic resistance (s $m^{-1}$); $\rho_a$ = air density (kg $m^{-3}$); c = correction factors of temperature on a well-watered, fully transpiring surface; k = coefficient for scaling grass reference ET ($ET_o$) to the maximum ET experienced by an aerodynamically rougher crop.

For this study, SSEBop monthly actual ET was acquired at 1 km spatial resolution from the U.S. Geological Survey Geo Data Portal (USGS GDP) (cida.usgs.gov). SSEBop analysis consisted of two components. First, monthly SSEBop ET was acquired for the area burned in 2013 by the Thompson Ridge Fire, pre- (2007–2013) and post-fire (2013–2014), to demonstrate the ability of the SSEBop algorithm to represent post-fire ET (detailed in Section 3.1). Second, after SSEBop ET was validated with the Thompson Ridge Fire, monthly SSEBop ET was acquired for the Las Conchas Fire area for 15 years from 2000 to 2014 (detailed in Sections 3.2 and 3.3).

### 2.2. Precipitation

The Parameter-elevation Regressions on Independent Slopes Model (PRISM) is based on elevation to approximate local climate components (PRISM Climate Group). It is derived from digital-elevation models, nearby weather station data, physiographic variables, proximity to coastlines, terrain complexity, and local temperature inversions (Daly et al., 1997). For this analysis and study domain, monthly precipitation data from WY 2001–2014 at 4 km resolution was acquired from the USGS GDP (cida.usgs.gov).

### 2.3. Ground-based ET – eddy covariance towers

Established in 1996, AmeriFlux consists of sites in North, Central and South America as a regional part of a global network – "FLUXNET" (Baldocchi, 2008). Currently, Fluxnet has more than 500 tower sites from approximately 30 regional networks, providing half-hourly to hourly measurements of $CO_2$, water, and energy fluxes and a unique opportunity to validate modeled processes.

Latent heat flux (LE) data from AmeriFlux was used to validate the performance of SSEBop ET in a burned area. Flux data was not available for the Las Conchas Fire, however, SSEBop ET was validated using another wildfire in the nearby region, the Valles Caldera National Preserve. Two AmeriFlux eddy covariance towers in two types of vegetation: Valles Caldera Mixed Conifer (US-Vcm) and Valles Caldera Ponderosa Pine (US-Vcp) were affected by the Thompson Ridge Fire in 2013 (Litvak, 2007a; 2007b). The soil burn severity for the mixed conifer and ponderosa pine towers were moderate and low, respectively. From LANDFIRE (detailed in Section 2.5), ponderosa pine woodland remained unchanged while the mixed conifer tower was reclassified as subalpine grassland after the fire (LANDFIRE, 2012, 2014). To validate pre- (2007–2013) and post-fire (2013–2014) SSEBop ET (Fig. 1), gap-filled 30-min LE tower data (W $m^{-2}$) from 2007 to 2014 were acquired and converted to ET in millimeters:

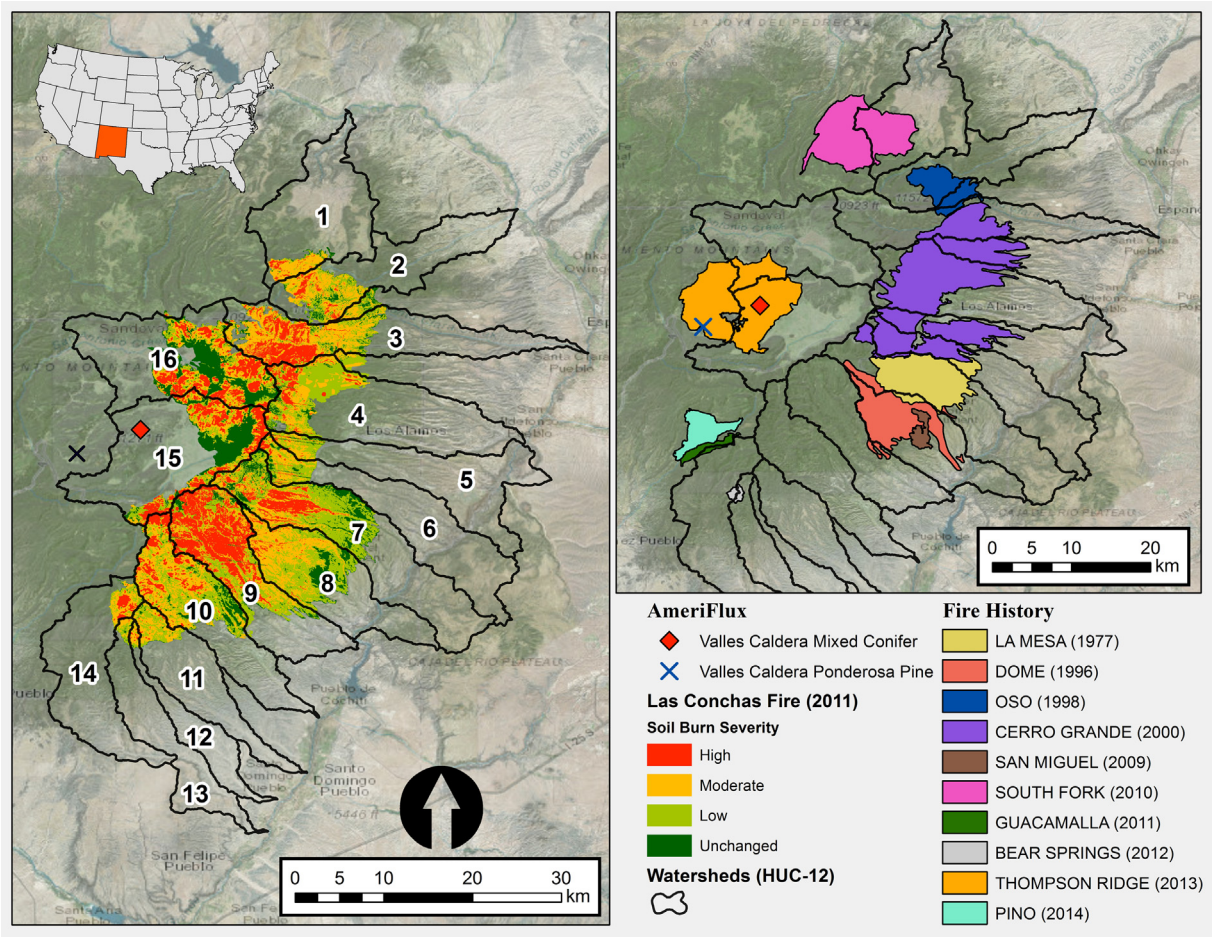


**Fig. 1.** (Left) Map of the Las Conchas Fire in New Mexico, U.S. HUC-12 watersheds (ID 1–16), the locations of the AmeriFlux stations, and spatial distribution of soil burn severity. (Right) Notable historical wildfires within the study region (extents of the Las Conchas Fire).

$$ET = \frac{LE}{\rho l_v} \quad (7)$$

where $l_v$ is latent heat of vaporization (2.45 MJ kg$^{-1}$) and $\rho$ is the density of water (1000 kg m$^{-3}$) (Mu et al., 2011; Senay, 2008; Velpuri et al., 2013). Ground-based LE data were aggregated to monthly data to match the resolution of SSEBop ET for comparison.

### 2.4. Soil burn severity

U.S. Department of Agriculture (USDA) Forest Service and U.S. Department of Interior derives metrics for soil burn severity from Landsat imagery. Burned Area Reflectance Classification (BARC) is based on the Normalized Burn Ratio (NBR) (8):

$$NBR = \frac{NIF - SWIF}{NIF + SWIF} \quad (8)$$

where *NIF* indicates Near-infrared and *SWIF* indicates short-wave infrared. The difference between pre- and post-fire *NBR* is known as dNBR, which represents a preliminary burn severity. BARC values are scaled from 0 to 255 (Parsons et al., 2010); low values represent low burned areas and values increase with soil burn severity (SBS). Initial thresholds are set as 0 to 75 for unchanged, 76 to 109 for low, 110 to 187 for moderate, and 188 to 225 for high burn regions (Parsons et al., 2010). This preliminary product is validated and adjusted through field measurements of ground cover, ash color and depth, soil structure, condition of roots, pre-fire vegetation, and water repellency for each SBS class. Generally almost all pre-fire ground cover, large trees, and surface organic matter are consumed in high SBS regions, leaving several centimeters in depth of white or grey ash. Moderate SBS indicates that up to 80% of the pre-fire ground cover is consumed. Scorched needles and leaves may remain in the canopy that will fall to the ground. Low SBS regions have surface organic layers that are not completely consumed. The canopy and understory vegetation are likely "green" and roots are generally similar to unburned conditions. Validated soil burn severity maps are available from the Remote Sensing Applications Center (https://www.fs.fed.us/eng/rsac/baer/). The Las Conchas Fire SBS map was acquired at 30 m resolution for this analysis.

### 2.5. Vegetation

LANDFIRE (LF) contains comprehensive maps and data describing vegetation, fuel, fire regimes, and ecological changes for the United States (Rollins, 2009). Existing vegetation type (EVT) is a data product derived by LF from NatureServe's Ecological Systems classification, alliances of the U.S. National Vegetation Classification, the National Land Cover Database, and LF specific vegetation types (LANDFIRE accessed 10 November 2017). For this analysis, three EVT layers (30 m resolution) were acquired for 2010, 2012, and 2014 (LANDFIRE, 2010, 2012, 2014). The 2010 and 2012 maps were used to observe general shifts in vegetation after the Las Conchas Fire, and the 2012 and 2014 maps were used for the Thompson Ridge Fire.

### 2.6. Study area

In June 2011, the Las Conchas Fire burned 634 km$^2$ in the Santa Fe National Forest and portions of the Valles Caldera National Preserve in the Counties of Sandoval, Los Alamo, and Rio Arriba, New Mexico (Fig. 1). It was the second largest wildfire in New Mexico and impacted 16 subwatersheds. The Valles Caldera is characterized as semi-arid, with seasonally snow-covered forest, where the main source of runoff is from snowmelt and spring rainfall (Liu et al., 2008). The elevation of the burned region ranged from 1570 to 3528 m. Based on the soil burn severity (SBS) classification, the Las Conchas Fire was classified as 30% low, 35% moderate, 21% high, and 14% unchanged (Fig. 1; RSAC, 2011). Unaffected percentages were areas within the watershed that were outside of the fire perimeter (Fig. 1). The vegetation within the Las Conchas Fire region in 2010 (LANDFIRE, 2010) consisted of approximately 75% conifer (a mix of ponderosa pine, douglas fir forest, and pinyon-juniper woodland), 14% hardwood (a combination of mixed conifer-oak forest and woodland), 4% shrubland (sagebrush, chaparral, and deciduous shrubland), and 2.5% grassland. In 2012, a year after the fire, the vegetation consisted of 52% conifer, 9% hardwood, 0.1% shrubland, and 32% grassland (LANDFIRE, 2012).

Sixteen subwatersheds (hydrologic unit code – 12) were affected (Fig. 1; Table 1). Rio Chiquito (ID 9) had the highest percentage of high SBS, whereas Outlet Borrego Canyon (ID 13) was minimally affected and used as a control watershed. There were several significant wildfires during the study period that may potentially influence this study and were considered during watershed selection and analysis (Fig. 1; Table 2).

## 3. Methods

### 3.1. AmeriFlux and SSEBop ET comparison – 2013 Thompson Ridge Fire

The comparison was conducted from 2007 to 2014 between ground-based ET and SSEBop ET for the Thompson Ridge Fire, which included a total of 77 pre-fire and 19 post-fire months.

**Table 1**
Characteristics of each watershed. High, moderate, low, and unchanged percentages. Unaffected percentages are defined as non-impacted regions within the HUC-12 watershed. The control watershed (ID 13, Outlet Borrego Canyon) is denoted by an*.

| ID | Name | High | Moderate | Low | Unchanged | Unaffected | Elevation (m) |
|---|---|---|---|---|---|---|---|
| 1 | Abiquiu Creek | 0.0% | 5.3% | 1.3% | 0.7% | 92.7% | 1870–3220 |
| 2 | Rio del Oso | 1.5% | 21.3% | 8.8% | 1.5% | 66.9% | 1760–3190 |
| 3 | Santa Clara Creek | 9.8% | 27.4% | 12.8% | 0.6% | 49.4% | 1700–3100 |
| 4 | Los Alamos Canyon | 6.3% | 8.3% | 19.3% | 1.0% | 65.1% | 1727–3050 |
| 5 | Canada Anacha – Rio Grande | 0.0% | 2.1% | 4.9% | 1.4% | 91.7% | 1660–3005 |
| 6 | Water Canyon – Rio Grande | 0.7% | 6.6% | 6.6% | 0.7% | 85.4% | 1724–2847 |
| 7 | Alamo Canyon – Rio Grande | 9.9% | 9.4% | 24.0% | 7.8% | 49.0% | 1628–2875 |
| 8 | Capulin Canyon–Rio Grande | 0.0% | 28.3% | 28.3% | 7.2% | 36.2% | 1664–2598 |
| 9 | Rio Chiquito | 40.4% | 12.6% | 20.5% | 4.0% | 22.5% | 1703–2767 |
| 10 | Peralta Canyon | 12.8% | 20.1% | 28.9% | 4.7% | 33.6% | 1675–2961 |
| 11 | Canon Santo Domingo | 0.0% | 15.7% | 7.8% | 0.0% | 76.5% | 1595–2559 |
| 12 | 130,202,010,603 (No Name) | 0.0% | 3.6% | 3.6% | 0.0% | 92.9% | 1590–2558 |
| 13* | Outlet Borrego Canyon | 0.0% | 1.0% | 3.1% | 0.0% | 95.8% | 1591–2501 |
| 14 | Headwaters Borrego Canyon | 2.0% | 5.4% | 0.7% | 0.7% | 91.2% | 1822–2700 |
| 15 | East Fork Jemez River | 12.6% | 7.4% | 3.7% | 13.7% | 62.6% | 2450–3313 |
| 16 | Headwaters San Antonio Creek | 9.7% | 13.5% | 10.3% | 17.3% | 49.2% | 2581–3088 |

**Table 2**
Notable historical wildfires within the study region in chronological order.

| Fire name | Month and Year | Area Burned ($km^2$) |
|---|---|---|
| La Mesa | June 1977 | 62 |
| Dome | April 1996 | 6.7 |
| Oso | June 1998 | 26 |
| Cerro Grande | May 2000 | 190 |
| San Miguel | July 2009 | 6.6 |
| South Fork | June 2010 | 69 |
| Las Conchas | June 2011 | 634 |
| Guacamalla | August 2011 | 6.3 |
| Bear Springs | June 2012 | 2.5 |
| Thompson Ridge | May 2013 | 97 |
| Pino | August 2014 | 18 |

Standard statistical metrics, correlation ($R^2$), mean bias error (MBE), and root mean squared error (RMSE) were used to evaluate the SSEBop ET product. Correlation ($R^2$) represented the degree of relationship between SSEBop ET and AmeriFlux ground-based ET. The root mean squared error (RMSE) was used to predict the accuracy between the SSEBop ET model and ground-based ET derived from AmeriFlux. Mean bias error (MBE) quantified the difference between SSEBop and Fluxnet ET. Results were also compared with previous studies at the unburned forest and grassland regions done by Senay et al. (2013), Velpuri et al. (2013), and Savoca et al. (2013).

### 3.2. Annual and seasonal ET – 2011 Las Conchas Fire

SSEBop monthly actual ET was analyzed at 1 km resolution from WY 2001–2014. To match the resolution of SSEBop ET, PRISM precipitation was disaggregated from 4 km to 1 km and was used as a proxy of available water and climate conditions before and after the fire. Annual precipitation and SSEBop ET for both pre- and post-fire were averaged within each watershed. To minimize the influence of precipitation on ET estimates, a ratio of ET to precipitation (ET/P) was calculated and statistically tested using a two-tail T-test ($\alpha < 0.05$) to identify watersheds with variations in the means due to the fire event. The SBS data were aggregated to 1 km resolution for comparison with SSEBop ET. Each ET pixel was associated with the following SBS levels: high, moderate, low, unchanged, and unaffected (not within the Las Conchas Fire perimeter). Within a watershed (Fig. 1; Table 1), the trends of ET with various SBS levels were investigated annually and seasonally (Fall (October-December), Winter (January-March), Spring (April-June), Summer (July-September)) before and after the fire.

### 3.3. Spatial evapotranspiration – 2011 Las Conchas Fire

Sixteen watersheds were analyzed and the current study highlights the evapotranspiration patterns for five watersheds: Outlet Borrego Canyon (ID 13; control watershed), Rio del Oso (ID 2; predominantly moderate SBS and unaffected), Rio Chiquito (ID 9; high SBS), Peralta Canyon (ID 10; primarily medium and low SBS), and Headwaters San Antonio Creek (ID 16; all SBS) to provide a range of burn severity conditions and minimize the influence from other wildfires (Table 2). Vegetation types were associated to the aggregated SBS and corresponding ET values. Three specific relations were investigated: 1) the ratio of post-fire ET (Dif.; Table 4) for each SBS and unaffected regions within a watershed (9); 2) the magnitude of change in ET ($\Delta$; Table 4) based on SBS when compared with unburned areas (10); 3) the percentage differences of the change in ET (%ET; Fig. 6) related to vegetation types and SBS within each watershed (11).

$$Dif. = \frac{X_{i_{post}} - X_{un_{post}}}{X_{un_{post}}} \quad (9)$$

$$\Delta = \frac{X_{i_{pre}} - X_{i_{post}}}{X_{un_{pre}} - X_{un_{post}}} \quad (10)$$

$$\%ET = \frac{X_{i_{pre}} - X_{i_{post}}}{X_{i_{pre}}} \quad (11)$$

where $X$ = ET (mm), $i$ denotes SBS classification (high, moderate, low).

## 4. Results

### 4.1. AmeriFlux and SSEBop comparison - 2013 Thompson Ridge Fire

To evaluate the performance of post-fire SSEBop, ET was compared with two AmeriFlux Towers located in Valles Caldera, which were burned by the Thomas Ridge Fire (May 2013). At the mixed conifer site, SSEBop had a pre-fire correlation of 0.78 and RMSE of 9.14 mm/month and a post-fire correlation of 0.56 and RMSE of 26.48 mm/month with AmeriFlux ET (Fig. 2a). The pre- and post-fire MBE were 22.58 and 13.3 mm/month, respectively, indicating that SSEBop overestimated before and after the Thompson Ridge Fire. At the ponderosa pine site, pre- and post-fire correlations were 0.77 and 0.74, with RMSE values of 18.19 and 25.46 mm/month, respectively (Fig. 2b). SSEBop underestimated at this site, where the pre-fire MBE was −8.7 mm/month and post-fire MBE was −17.95 mm/month (Fig. 2b), which was in contrast to the mixed conifer site.

### 4.2. Annual and seasonal ET – 2011 Las Conchas Fire

The pre- and post-fire precipitation and ET were estimated for each watershed within the Las Conchas Fire (Fig. 3; Supplementary Figs. 1–16). Five watersheds (ID 3, ID 4, ID 8, ID 15, and ID 16) had an annual ET that was greater than precipitation before the fire and the ET decreased below the total precipitation after the fire. Two of the five watersheds had an annual post-fire ET that was greater than the post-fire precipitation (ID 1 and ID 16). Post-fire ET decreased approximately 60–250 mm/yr in all watersheds (Fig. 3).

The monthly ET/P for all watersheds ranged from 0.4 to 2.5 (Supplementary Figs. 1–16) and were sensitive to annual precipitation and the fire. In WY 2002, the ratios of ET/P were consistently larger than the other water years for all watersheds. Following the Las Conchas Fire (2011), 2012 and 2013 had smaller ET/P ratios (Supplementary Figs. 1–16). The two-tail $t$-test of annual ET/P indicated that 9 of the 16 watersheds (15 affected and the control watershed) were statistically different after fire at a 0.05 significance level (Table 3).

Outlet Borrego Canyon (ID 13; control watershed) had a pre-fire (WY 2001–2011) average annual precipitation of 549 (±96) mm and annual ET of 442 (±45) mm. The annual post-fire (WY 2012–2014) precipitation was 482 (±29) mm and post-fire ET was 377 (±20) mm. The relationship of ET and P (ET/P) decreased by 0.03 between the pre- and post-fire periods (Table 3). In general, ET/P following the wildfire was constant with a minimal increase of 0.02 from 2011 to 2014 (Fig. 4). Seasonally, the ET difference between pre- and post-fire was greatest during April to June by approximately 14 mm/month (Fig. 5; left column), while October–March had a minimal decrease of 3 mm/month (not shown in Fig. 5).

Rio Chiquito (ID 9; high severity watershed) had a mean annual precipitation before the Las Conchas Fire of 612 (±120) mm and post-fire precipitation of 552 (±45) mm. The annual pre-fire ET average was 565 (±57) mm, which substantially decreased after the fire to 395 (±11) mm. A decline in ET/P of 0.21 for 2 years following the fire was caused by the increase of precipitation and decrease of ET (Supplementary Fig. 9; Fig. 4). The difference of

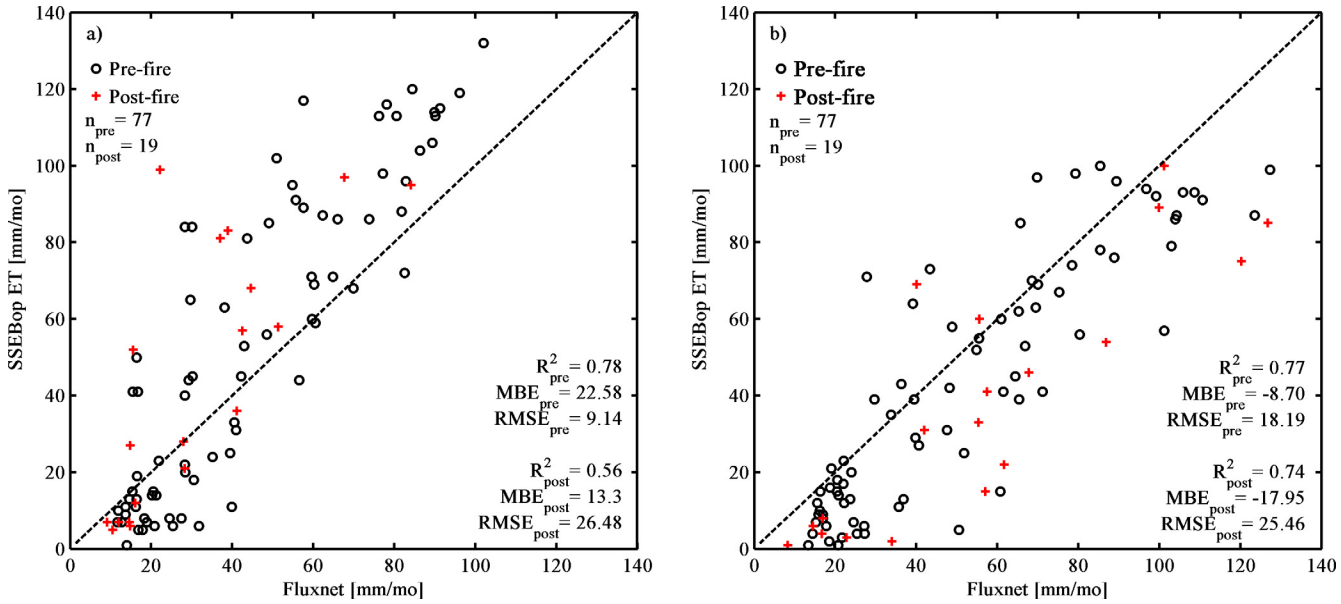


**Fig. 2.** Comparison between SSEBop ET and eddy covariance AmeriFlux towers at the Valles Caldera a) mixed conifer and b) ponderosa pine sites from 2007 to 2014. A 1:1 line, correlation (R), mean bias error (MBE), and root mean squared error (RMSE) are noted (with units of mm/month). The number (n) of data points for pre- and post-fire are 77 and 19 respectively.

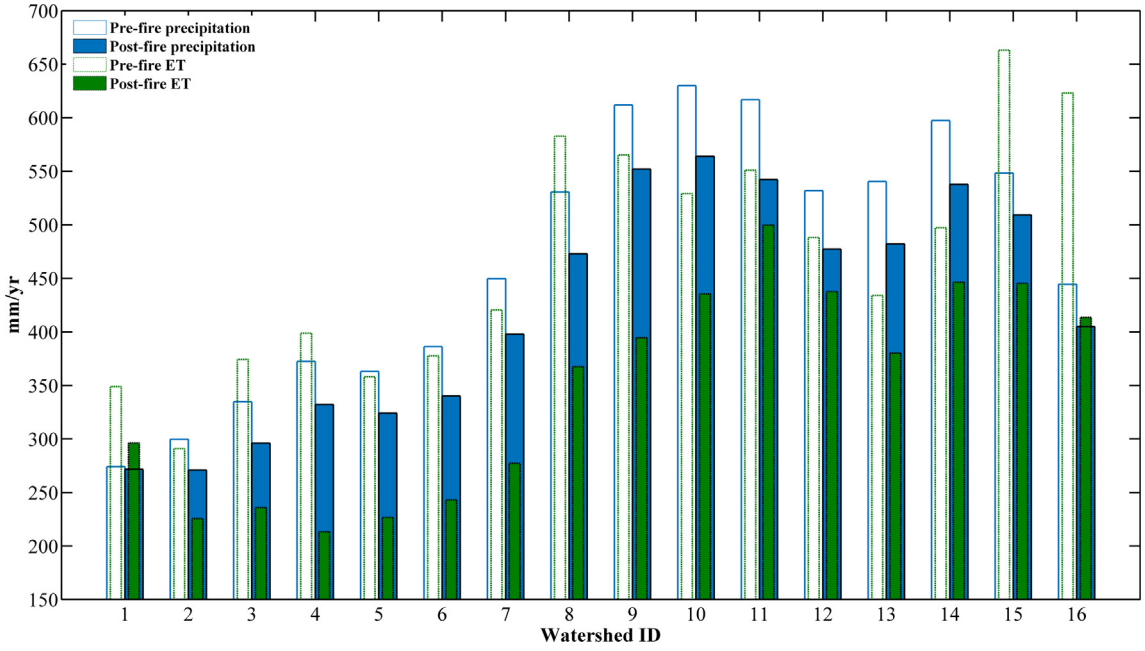


**Fig. 3.** Spatially averaged total annual precipitation and ET (in mm/yr) for all watersheds (shown by watershed ID).

ET/P averages was 0.24 (p-value = 0.026), indicating that the pre- and post-fire ET/P were statistically different. Seasonally, there was a minimal decrease of ET (4 mm/month) in the winter and spring. A greater decrease of ET during the summer seasons was noted for all burn severity types (30 mm/month) (Fig. 5). Within Rio Chiquito, the highest annual relative difference of ET (burned versus unaffected areas) was 51.6% in the low severity regions, while there was only a relative change of 14.6% in the high burn severity areas (Table 4).

Headwaters San Antonio Creek (ID 16; mixed soil burn severities) had a mean pre-fire precipitation of 453 (±90) mm from WY 2001–2011 and a similar average post-fire precipitation of 402 (±32) mm from WY 2012–2014. However, the post-fire annual ET decreased by 200 mm for the whole watershed, from 634 (±42) mm to 437 (±24) mm. Consequently, ET/P was reduced by 0.51 (1.4 to 0.9) immediately following the wildfire and was statistically different (Fig. 4; Table 3). Similar to the other watersheds, the highest difference in pre- and post-fire ET was between April to June, where a decrease of 24, 44, 49, and 57 mm/month for unaffected, low, moderate, and high severity areas was noted respectively (Fig. 5).

Peralta Canyon (ID 10; moderate and low burn severity watershed) had a pre- and post-fire annual precipitation of 639 (±30) mm and 574 (±29) mm, respectively. There was a notable decrease of approximately 100 mm of annual ET after the fire, from 538 (±40) mm to 438 (±41) mm. The trends of ET and precipitation following the fire (2011–2014) were similar, resulting in a constant

**Table 3**
Monthly average precipitation (P), evapotranspiration (ET), standard deviation (σ), and mean ET to P (ET/P) for pre- and post-fire years for each watershed. Watershed ID with an * have pre- and post-fire means of ET/P that are statistically different at α = 0.05. The control watershed (ID 13, Outlet Borrego Canyon) is denoted by a+.

| | P [mm] | | ET [mm] | | σ of ET | | Mean of ET/P | | |
|---|---|---|---|---|---|---|---|---|---|
| Watershed ID | Pre- | Post- | Pre- | Post- | Pre- | Post- | Pre- | Post- | P-value |
| 1 | 274 | 272 | 349 | 296 | 34 | 38 | 1.36 | 1.09 | 0.0528 |
| 2* | 300 | 271 | 291 | 225 | 43 | 43 | 1.03 | 0.83 | 0.0442 |
| 3* | 335 | 296 | 374 | 236 | 36 | 34 | 1.17 | 0.80 | 0.0054 |
| 4* | 372 | 332 | 399 | 213 | 32 | 32 | 1.11 | 0.65 | 0.0259 |
| 5 | 363 | 324 | 358 | 227 | 36 | 25 | 1.01 | 0.71 | 0.0573 |
| 6* | 386 | 340 | 378 | 243 | 47 | 34 | 1.00 | 0.73 | 0.034 |
| 7* | 450 | 398 | 420 | 277 | 51 | 39 | 0.96 | 0.70 | 0.0137 |
| 8* | 540 | 473 | 600 | 377 | 44 | 36 | 1.14 | 0.78 | 0.007 |
| 9* | 612 | 552 | 565 | 395 | 47 | 45 | 0.96 | 0.72 | 0.0264 |
| 10 | 639 | 574 | 538 | 438 | 39 | 41 | 0.87 | 0.78 | 0.178 |
| 11 | 625 | 553 | 559 | 493 | 36 | 36 | 0.93 | 0.92 | 0.991 |
| 12 | 540 | 478 | 495 | 434 | 27 | 27 | 0.94 | 0.92 | 0.646 |
| 13+ | 549 | 482 | 442 | 377 | 40 | 39 | 0.82 | 0.79 | 0.43 |
| 14 | 607 | 538 | 504 | 445 | 33 | 32 | 0.86 | 0.83 | 0.62 |
| 15* | 557 | 512 | 676 | 471 | 40 | 49 | 1.27 | 0.88 | 0.0074 |
| 16* | 453 | 402 | 634 | 437 | 38 | 40 | 1.47 | 1.03 | 0.0157 |

ET/P that resembled the control watershed (Supplementary Fig. 10; Fig. 4). The change of mean annual ET/P before and after the fire was 0.09 and not significant at a 5% level (Table 3). Seasonally, ET decreased during April to September for the whole watershed: 20 mm/month for unaffected, 23 mm for moderate, and 28 mm/-month for low burn severity areas (Fig. 5).

In Rio del Oso (ID 2; unaffected and mostly moderate severity watershed), the average annual precipitation before and after the fire was 300 (±82) and 271 (±24) mm respectively. The pre-fire averaged annual ET from unaffected areas was 349 (±35) mm and the post-fire annual ET was 296 (±31 mm). Similar to Headwaters San Antonio Creek watershed, the annual ET/P significantly declined immediately after the fire, from 1.3 to 0.8 (Supplementary Fig. 2; Fig. 4). The moderately burned area pre-fire annual ET was 328 (±41) mm and the mean post-fire annual ET was 230 (±36) mm. Similar to the control watershed, the largest decrease in ET occurred between April to June, with 13 mm/month for moderate and 7 mm/month for unaffected areas. During the summer seasons, there was a large decrease of 21.7% in ET in moderate areas and 13.0% in unaffected areas within Rio del Oso (Fig. 5).

### 4.3. Spatial evapotranspiration – 2011 Las Conchas Fire

Within each watershed, the regions unaffected by the fire were compared to each SBS level to observe the change in post-fire ET after the Las Conchas Fire. Lower annual post-fire ET in high soil burn severities were observed compared to the unaffected (Rio Chiquito), low (Headwaters San Antonio Creek), and moderate (Rio del Oso) severities. These watersheds contained the most high and moderate SBS areas and the largest declines in ET (Table 4). While Peralta Canyon had larger post-fire ET in high and moderate burned areas compared to low burn severity areas (Table 4).

Rio del Oso showed the smallest difference in annual ET for all SBS areas (Table 4). It had a difference of 102 mm between pre- and post-fire annual ET in the high SBS, 98 mm in the moderate SBS, 91 mm in the low SBS, and 65 mm in the unaffected areas. Post-fire ET was 20% lower in high SBS, 17% lower in moderate SBS, 11% lower in low SBS when compared to unaffected areas (Table 4). Similarly, Headwaters San Antonio Creek generally decreased, in which the average post-fire annual ET was 24% lower in high SBS, and 15% lower in moderate SBS. Annual ET in Rio Chiquito had the largest percentage differences across various SBS; high, moderate, and low SBS areas had lower ET than the unaffected regions by 36, 34, and 29%. Contrary to the above watersheds, Peralta Canyon post-ET difference was greatest in low SBS regions (22%) and smallest in high SBS areas (19%). High SBS areas had a greater post-fire average annual ET (405 mm) than low burn severity (390 mm) (Table 4).

The ratio (Δ) between the ET difference of SBS regions and unaffected regions (10) showed the magnitude of decrease of each watershed. Rio del Oso and Headwaters San Antonio Creek were similar, where ET had a larger magnitude of decrease with increasing SBS (Table 4). The Δ's for Rio del Oso ranged from 1.4 to 1.57, whereas Δ's for Headwaters San Antonio Creek ranged from 1.97 to 2.57, the highest Δ values amongst all watersheds. Although Rio Chiquito had the greatest ratio difference of ET within the watershed, the low SBS had an unexpectedly higher decline of ET (602 to 375 mm) than the other SBS levels. Further, the Δ's from Peralta Canyon showed mixed results; the magnitude of decrease was lowest in moderate SBS areas (1.02) and highest in high SBS areas (1.37).

The percentage difference (11) between the pre- and post-fire ET (%ET) estimates was noted with respect to the vegetation within a SBS region (Fig. 6). In the burned regions of the four fire-affected watersheds, all major vegetation types (conifer, hardwood, and shrubland) decreased except grassland. The amount of vegetation decreased from −3.8% to −62.7% in conifer, −0.2 to −24.4 in hardwood, and −0.1% to −3.7% in shrubland. The increase in grassland across all burn severities was approximately 4.5% to 69.1%. The sum of the decrease in conifer and hardwood closely represented the increase of grassland within all affected regions, however there was no direct relation between the percentage change in ET and amount of vegetation converted to grassland (Fig. 6). The%ET ranged from –22.6% to −51.2% (high), −20.4% to −39.9% (moderate), and -18.3% to -44.8% (low) across the watersheds. At unburned regions of the fire-affected watersheds, minimal changes across vegetation types and a slight decrease in%ET (−14.7% to 23.6%) were observed (Fig. 6). At Outlet Borrego Canyon, the control watershed, the amount of conifer decreased by 27.5%, 3.7, and 0.7 at moderate, low, and unburned regions respectively. Similar to other watersheds, the amount of grassland increased by 27.5%, 3.9%, and 0.7% in moderate, low, and unburned areas, respectively. The%ET decreased minimally and ranged from -5.6% to -12.8% within the watershed.

## 5. Discussion

### 5.1. AmeriFlux and SSEBop comparison – 2013 Thompson Ridge Fire

SSEBop ET was evaluated under post-fire conditions within the Thompson Ridge Fire. In general, SSEBop performed well compared

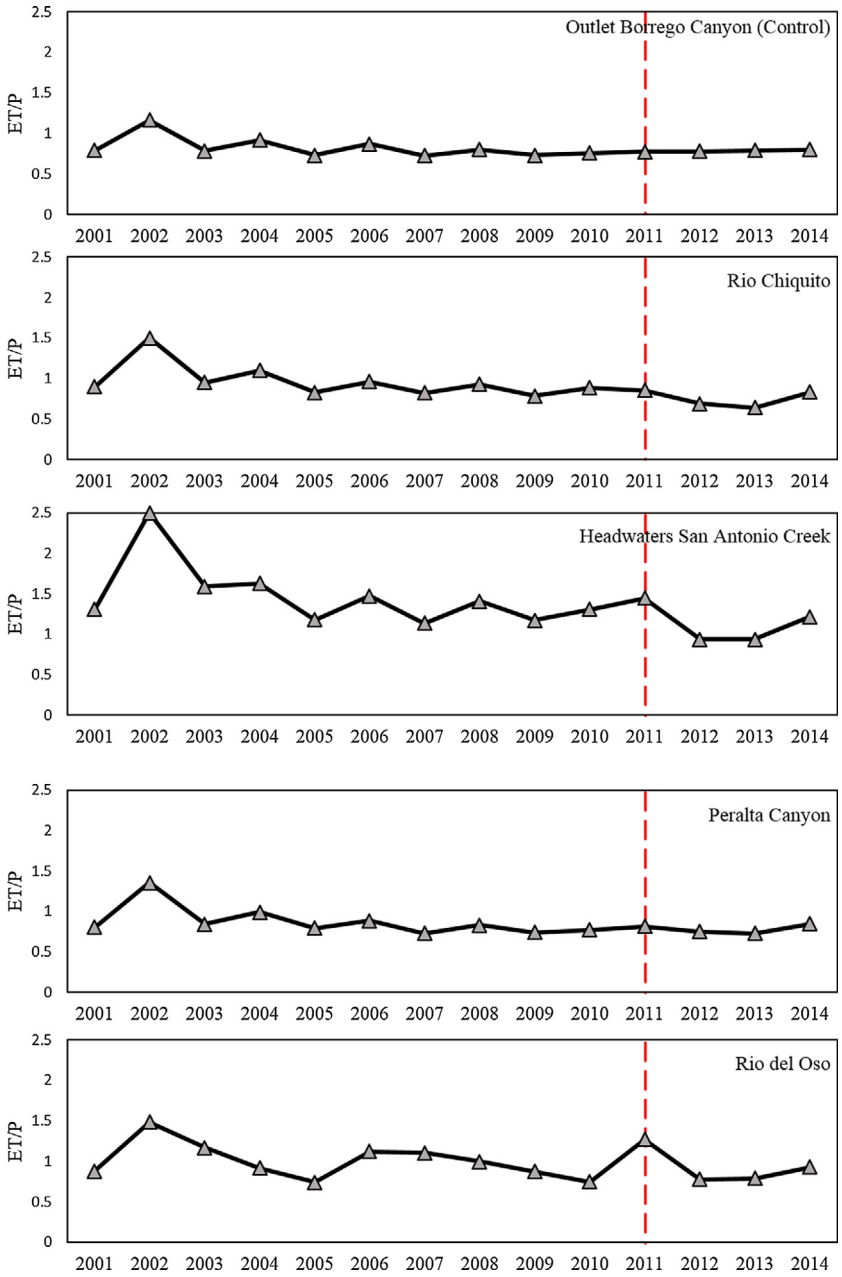


**Fig. 4.** Annual ET/P from water year 2001–2014 for Outlet Borrego Canyon, Rio Chiquito, Headwaters San Antonio Creek, Peralta Canyon, and Rio del Oso watersheds. Red dashed line indicates Las Conchas Fire. (For interpretation of the references to color in this figure legend, the reader is referred to the web version of this article.)

to the AmeriFlux towers, where the pre- and post-fire correlations ranged from $R^2$ = 0.56–0.78 and the RMSE ranged from 9 to 26 mm/month (Fig. 2). Generally, the post-fire values of SSEBop and AmeriFlux fall within the range of the pre-fire values, however, there were less data points from the post-fire period (19 months), which contributes to uncertainty in the correlation. In the mixed conifer site, SSEBop tended to overestimate ET by 13 to 22 mm/month (Fig. 2a), while the ponderosa pine site underestimated by 8.7 to 18 mm/month (Fig. 2b). These differences are attributed to the variability of vegetation types within the LANDFIRE conifer classification, systematic errors from the model algorithm, MODIS pixel size (heterogeneous composition within the pixel), and uncertainty in AmeriFlux measurements (Chen et al., 2016; Velpuri et al., 2013). The $R^2$ values from this analysis (0.56–0.78) are similar to those reported by Savoca et al. (2013), where SSEBop and Fluxnet correlations ranged from 0.75 to 0.82 for grassland and forests. Additionally, the root mean squared error (9–26 mm/month) in this analysis is similar to Senay et al. (2013) and performs better than the observed RMSE (25–32 mm/month) in eddy covariance towers by Velpuri et al. (2013). Based on these observations, the SSEBop ET product provides reasonable pre- and post-fire ET estimates and is readily available without the need to perform image post-processing (i.e. cloud filtering or hot and wet pixel selection), which allows an efficient analysis of spatial and temporal patterns of monthly ET.

### 5.2. Annual and seasonal ET – 2011 Las Conchas Fire

There was a statistically significant decrease in ET, which was attributed primarily to the Las Conchas Fire (Fig. 3). A control watershed and the addition of precipitation provided context for the impacts of climate on the observed ET processes. The annual

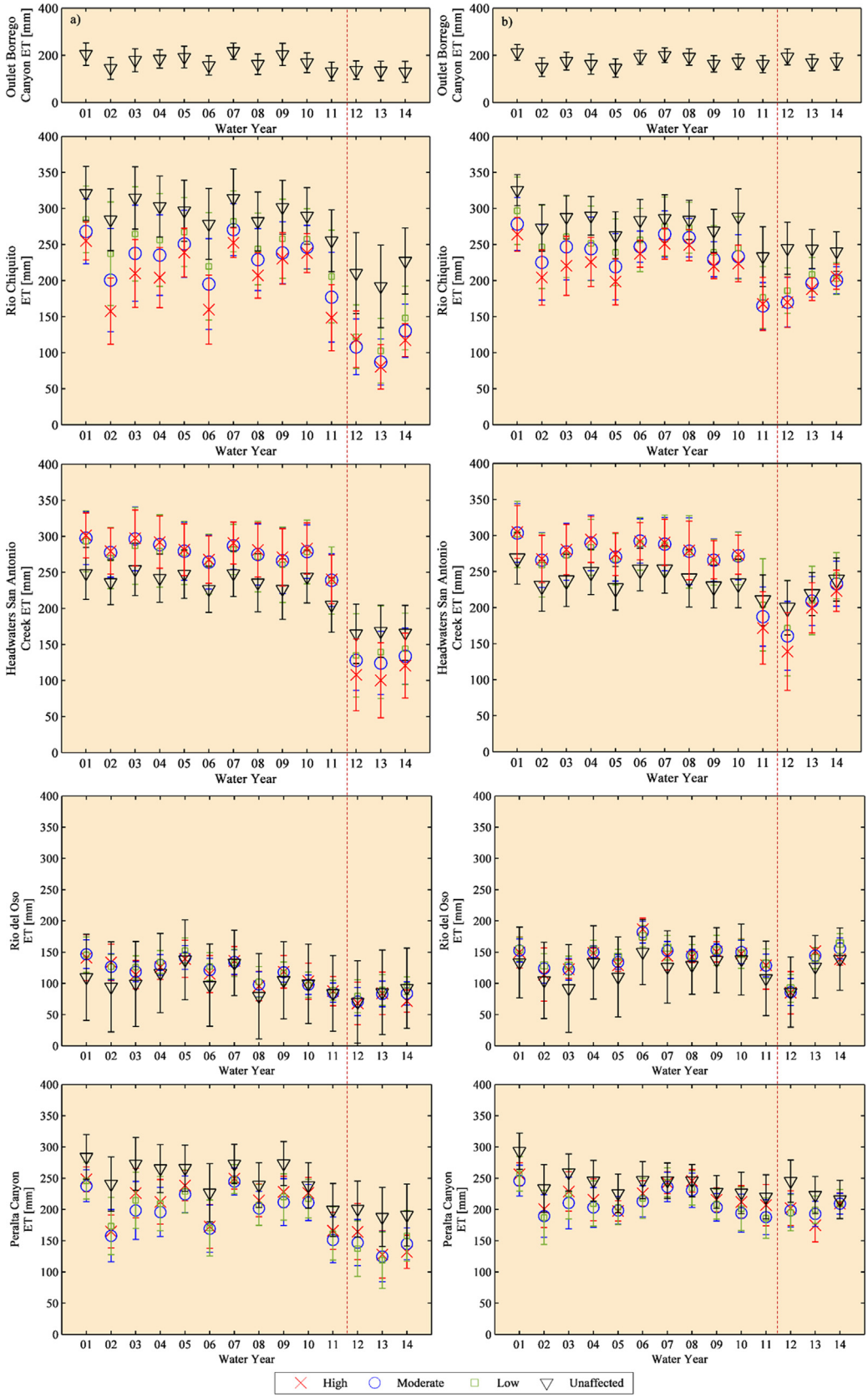


**Fig. 5.** Seasonal ET for Outlet Borrego Canyon (control watershed) and watersheds that represent various burn severity levels: Rio Chiquito (high SBS), Headwaters San Antonio Creek (all SBS), Rio del Oso (predominantly moderate SBS and unaffected), and Peralta Canyon (primarily moderate and low) for April–June (Spring; left column) and July–September (Summer; right column). October–March data not shown (Fall and Winter). The vertical red line indicates the Las Conchas Fire. (For interpretation of the references to color in this figure legend, the reader is referred to the web version of this article.)

**Table 4**
Annual pre- and post-fire ET for each soil burn severity (high, moderate (mod), low, unaffected (UnA)) within for Rio Chiquito, Headwaters San Antonio Creek, Peralta Canyon, and Rio del Oso. *Ratio (Dif.) between post-fire ET for each SBS with respect to the unaffected region for each watershed (9). **The magnitude of change in ET ($\Delta$) at a burn severity level and the change of the unaffected region within each watershed (10).

| SBS | Pre | Post | Dif.* | $\Delta$** |
|---|---|---|---|---|
| | | Rio Chiquito | | |
| high | 510 | 339 | 36% | 1.15 |
| mod | 559 | 349 | 34% | 1.41 |
| low | 602 | 375 | 29% | 1.52 |
| unA | 679 | 530 | N/A | N/A |
| | | Headwaters San Antonio Creek | | |
| SBS | Pre | Post | Dif.* | $\Delta$** |
| mod | 679 | 375 | 15% | 2.24 |
| low | 671 | 403 | 9% | 1.97 |
| unA | 577 | 441 | N/A | N/A |
| | | Peralta Canyon | | |
| high | 523 | 405 | 19% | 1.37 |
| mod | 482 | 394 | 21% | 1.02 |
| low | 490 | 390 | 22% | 1.16 |
| unA | 586 | 500 | N/A | N/A |
| | | Rio del Oso | | |
| high | 324 | 222 | 20% | 1.57 |
| mod | 328 | 230 | 17% | 1.51 |
| low | 336 | 245 | 11% | 1.40 |
| unA | 342 | 277 | N/A | N/A |

ET for the control watershed (ID 13) decreased by 13.6% from the pre- to post-fire period, which was attributed to the declines of precipitation (Fig. 4) and two small fires (Bear Springs Fire 2012 and 2014) that burned a total of 1.6% of the watershed. However, the trend of ET/P following the fire remained relatively constant, which was expected in the control watershed as the relation between ET and P was not altered, highlighting altered ET regimes in burned watersheds. In six of the burned watersheds, ET was greater than precipitation before the fire (Section 4.2; Fig. 3), where antecedent conditions such as groundwater storage and snow processes may contribute additional available water for evapotranspiration processes. The ET/P noticeably increased in WY 2002 due to lower precipitation across all burned watersheds (Supplementary Figs. 1–16), this demonstrates that there was an availability of water for vegetation transpiration processes. Other uncertainties in this ET analysis can include errors from the SSEBop algorithm, where errors of each variable in the model may contribute up to an overall error of 20% (Chen et al., 2016).

Burn severity also influenced the observed temporal patterns of ET. Prior to the Las Conchas Fire, ET/P was relatively constant for all the watersheds. There was an observed decline in ET/P for the more severely burned watersheds following WY 2011, despite increased annual precipitation (Supplementary Figs. 1–10, 15 and 16). The burned watersheds had similar precipitation patterns to the control watershed (Outlet Borrego Canyon) from WY 2001–2014, yet there was still an observed decrease in post-fire annual ET by approximately 97–352 mm per year (Fig. 3). Of the 16 watersheds analyzed (15 affected and the control watershed), nine watersheds (ID 3–9, 15–16) had statistically different ($\alpha = 0.05$) mean annual post-fire ET. Thus, the decrease in post-fire ET is attributed to the wildfire induced landscape changes rather than the amount of available water from precipitation, snowmelt, and groundwater supplies. The observations from the current research corresponds with Montes-Helu et al. (2009), who noted that sensible and latent heats (energy associated with ET) were lower for 10 years after wildfire. The fire-induced vegetation change (i.e. transformation of ponderosa pine to grassland) reduced the availability of energy for heating the air, soil, and evaporating water and limits evapotranspiration (Montes-Helu et al., 2009).

The observed annual and seasonal changes in ET trends corroborates with previous studies. The 120 mm/yr decrease in the average annual ET for the entire area affected by the Las Conchas (Fig. 3) is similar to observations from Dore et al. (2010), who noted that post-fire ET was lower for 10–11 years after fire by 76–116 mm/yr. Sánchez et al. (2015) observed a decrease in ET by 1 mm/day after the fire, which is comparable to the seasonal decrease of roughly 13–57 mm/month observed in this study. The range observed in this study is due to varying burn severity. Sánchez et al. (2015) and Montes-Helu et al. (2009) noted that unburned ET (estimated by latent heat fluxes) were greater than burned ET from mid-April to December, and the largest differences occurred in May and July. Comparable seasonal patterns in ET are observed during this 14 year study period (Fig. 5) and are similar to ecosystem processes modeled by Atchley and Maxwell (2011), who showed that canopy loss and decreased shading in riparian areas increase surface evaporation, decrease transpiration, and results in an overall decrease in ET.

### 5.3. Spatial ET – 2011 Las Conchas Fire

Evapotranspiration trends vary spatially after wildfire and are impacted by burn severity. As hypothesized, higher SBS areas generally had greater decreases in ET (Table 4, Rio Chiquito, Headquarters San Antonio Creek, and Rio del Oso Watersheds). Field-based measurements in a mixed eucalypt forest by Nolan et al. (2014) observed that the average ET was 41% lower in high burn severity (662 mm/yr) and 9% lower in moderate burn severity (1066 mm/yr) compared to unburned forests with ET of 1097 mm/yr following the Black Saturday fires in Melbourne, Australia. Although the vegetation type cannot be directly compared, the ET difference in this study (Table 4; Dif.) following the Las Conchas Fire is similar. Dore et al. (2010) observed annual ET differences in ponderosa pine forests in Flagstaff, Arizona after a wildfire. The fire destroyed all trees and transformed the site to grasses, forbs, and shrubs. Post-fire ET was lower (365 ± 3 mm in 2006, 441 ± 15 mm in 2007) compared to an unburned site (481 ± 3 mm in 2006, 525 ± 12 mm in 2007) and resulted in approximately 12%–30% lower ET (Dore et al., 2010; 2012). This study also noted a shift in vegetation type from conifer to grassland after the Las Conchas Fire (Fig. 6) and a corresponding decrease in ET. The sum of the decrease in conifer and hardwood closely represented the increase of grassland within all affected regions, however the percentage

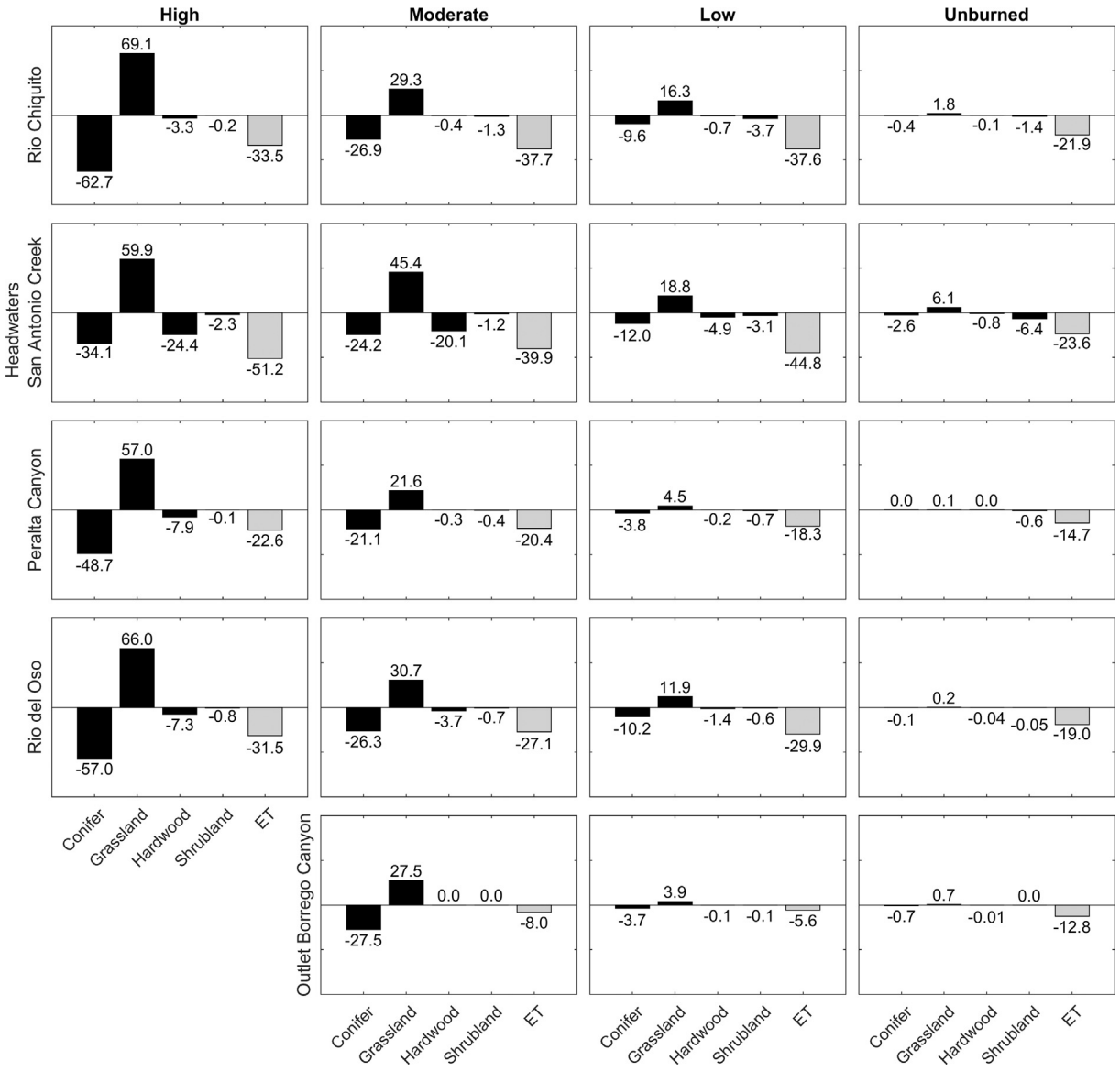


**Fig. 6.** Percentage difference in pre- and post-fire ET (% ET) and the difference of total vegetation from 2010 to 2012 for high, moderate, low, and unburned SBS within Rio Chiquito, Headwaters San Antonio Creek, Peralta Canyon, Rio del Oso, and Outlet Borrego Canyon watersheds. *No high burn regions in Outlet Borrego Canyon watershed.

change in ET did not have a direct relationship to the amount of vegetation converted to grassland (Fig. 6). The%ET (Fig. 6) is similar to Dore et al. (2010), but the current study provides more insight into patterns related to varying burn severity.

Utilizing remote sensing models can improve the quantification and analysis of post-fire ET at greater spatial and temporal scales. Observations from previous ground-based studies were limited by the number of field measurements and data sets. Sánchez et al. (2015) investigated a total of 15 satellite images, which may not fully capture seasonal and annual patterns in vegetation and ET. Using SSEBop 1 km, monthly ET from WY 2001–2015 for an entire burned region augments traditional analyses and improves our understanding of spatial and temporal variability after wildfire. Furthermore, the coupling of vegetation and remotely sensed ET can benefit post-fire runoff modeling, especially in catchments where actual ET is not dominated by equilibrium (Zhou et al., 2013). It is important to note that there are potential errors and uncertainty that may arise from aggregating burn severity from 30 m to 1 km pixels to match the resolution of SSEBop, which may misclassify some of the burn severities. Due to the size and number of watersheds analyzed in this study, the potential effect of misclassified burn areas is expected to be minimal.

### 5.4. Further implications

Utilizing remote sensing techniques can improve our ability to assess relative changes in ET after large wildfires at higher temporal resolutions. Although there are limitations and associated uncertainties with satellite-based estimates, this study is the first to apply an ET product at high spatial and temporal resolution to understand the relative impacts of wildfire on ET processes with respect to burn severity and vegetation type. These results have significant implications for water resources, provide insight into post-fire ET trends, and advances remote sensing for disturbance applications. Approximately 20–50% of the Rio Grande River in New Mexico is depleted due to riparian ET (Dahm et al., 2002). The current study estimates a decrease of approximately 120 mm/year within all the watersheds affected by the Las Conchas

Fire, which is about 10–16% of the average annual growing season ET (74–122 cm/yr; Dahm et al., 2002) in the Rio Grande region. This can have substantial impacts on regional water supplies, especially as large, catastrophic wildfires can potentially augment runoff available for downstream ecological communities and urban populations. However, there are also potentially negative impacts on water quality such as increased suspended sediment transport and increased total nitrogen, phosphorus, and heavy metal (Fe, Mn, As, Cr, Al, Ba, and Pb) concentrations (Smith et al., 2011). In light of ongoing drought and increasing wildfire activities, there is not only potential to degrade air and water quality, change biochemical processes and nutrient cycling, and alter watershed processes, but also potential to alter the long-term exchange between water and energy fluxes (Choromanska and DeLuca, 2002; Lane et al., 2006; Kinoshita and Hogue, 2011; Nolan et al., 2014; De Sales et al., 2015). Therefore, it is critical to predict and quantify post-fire watershed processes for ecosystem and resources management in semi-arid landscapes. Declines in streamflow following wildfire have also been documented because of antecedent soil moisture conditions and drought (Feikema et al., 2013; Nolan et al., 2015), suggesting a nonlinear correspondence of ET and surface runoff. Considering the emerging wildfire and drought nexus, there is a need to further investigate the threshold between the hydrologic components of the water balance, physical, and climactic factors on a region's resistance and recovery to disturbance. For example, the magnitude of influence from ET recovery on streamflow as a function of seedling regeneration and rates of transpiration from surviving trees following wildfires at regional scales requires further investigation.

## 6. Conclusion

This research investigates evapotranspiration after the Las Conchas Fire using remote sensing models and techniques to improve our understanding of spatial and temporal ET processes. First, we observed that the Operational Simplified Surface Energy Balance (SSEBop) ET Model can be suitable for pre- and post-fire analysis based on a comparison with ground-based observations (AmeriFlux). Second, annual and seasonal ET trends were altered after fire. Compared to pre-fire ET, the average post-fire annual ET decreased from 102.6 to 352.2 mm/yr, 97.2–303.9 mm/yr, and 90.9–267.7 mm/yr in high, moderate, and low SBS. The most prominent decrease in ET was during the summer, with 13–57 mm/month, despite regular summer monsoon storms. Third, we compared post-fire ET between various soil burn severities and unaffected areas. Generally, post-fire ET was 19.9–36.1%, 15–34.1%, and 8.7–29.1% lower in high, moderate, and low SBS areas, respectively, for all the watersheds within our study domain. Lastly, a shift of vegetation from mostly conifer to grassland was observed, which resulted in a general decrease in ET from −18 to −51%. This work has significant implications for water resources and encourages the integration of remote sensing techniques with traditional methods to enhance our knowledge of the complex hydrologic interactions in a disturbed environment. As wildfire activities increase through anthropogenic activities and climate change, understanding post-fire ET patterns can improve modeling of hydrological responses following wildfires in semi-arid landscapes.

## Acknowledgement

This research was supported by NASA Headquarters under the NASA Earth and Space Science Fellowship Program (16-EARTH16F-233). The authors would like to thank Dr. Tim McVicar, Dr. Patrick Lane, and three anonymous reviewers for their insightful comments and reviews.

## Appendix A. Supplementary data

Supplementary data associated with this article can be found, in the online version, at https://doi.org/10.1016/j.jhydrol.2018.02.023.

## References

Allen, R., Pereira, L., Smith, M., Raes, D., Wright, J., 2005. FAO-56 dual crop coefficient method for estimating evaporation from soil and application extensions. J. Irrig. Drain Eng. https://doi.org/10.1061/(ASCE) 0733-9437 (2005) 131:1(2), 2-13.

Allen, R.G., Tasumi, M., Trezza, R., 2007. Satellite-based energy balance for mapping evapotranspiration with internalized calibration (METRIC)—Model. J. Irrig. Drain. Eng. 133 (4), 380–394.

Atchley, A.L., Maxwell, R.M., 2011. Influences of subsurface heterogeneity and vegetation cover on soil moisture, surface temperature and evapotranspiration at hillslope scales. Hydrogeol. J. 19 (2), 289–305.

Baldocchi, D., 2008. 'Breathing' of the terrestrial biosphere: lessons learned from a global network of carbon dioxide flux measurement systems. Australian J. Bot. 56 (1), 1–26.

Bart, R.R., 2016. A regional estimate of postfire streamflow change in California. Water Resour. Res. 52 (2), 1465–1478.

Bastiaanssen, W.G., Menenti, M., Feddes, R.A., Holtslag, A.A.M., 1998. A remote sensing surface energy balance algorithm for land (SEBAL). 1 Formulation. J. Hydrol. 212, 198–212.

Benavides-Solorio, J., MacDonald, L.H., 2001. Post-fire runoff and erosion from simulated rainfall on small plots Colorado front range. Hydrol. Process. 15 (15), 2931–2952.

Bonan, G.B., 2008. Forests and climate change: forcings, feedbacks, and the climate benefits of forests. Science 320 (5882), 1444–1449.

Brooks, M.L., D'antonio, C.M., Richardson, D.M., Grace, J.B., Keeley, J.E., DiTomaso, J. M., Hobbs, R.J., Pellant, M., Pyke, D., 2004. Effects of invasive alien plants on fire regimes. BioScience 54 (7), 677–688.

Chen, M., Senay, G.B., Singh, R.K., Verdin, J.P., 2016. Uncertainty analysis of the Operational Simplified Surface Energy Balance (SSEBop) model at multiple flux tower sites. J. Hydrol. 536, 384–399.

Choromanska, U., DeLuca, T.H., 2002. Microbial activity and nitrogen mineralization in forest mineral soils following heating: evaluation of post-fire effects. Soil Biol. Biochem. 34 (2), 263–271.

Covington, W.W., Moore, M.M., 1994. Post settlement changes in natural fire regimes and forest structure: ecological restoration of old-growth ponderosa pine forests. J. Sust. For. 2 (1–2), 153–181.

Dahm, C.N., Cleverly, J.R., Allred Coonrod, J.E., Thibault, J.R., McDonnell, D.E., Gilroy, D.J., 2002. Evapotranspiration at the land/water interface in a semi-arid drainage basin. Freshwater Biol. 47 (4), 831–843.

Dale, V.H., Joyce, L.A., McNulty, S., Neilson, R.P., Ayres, M.P., Flannigan, M.D., Hanson, P.J., Irland, L.C., Lugo, A.E., Peterson, C.J., Simberloff, D., 2001. Climate change and forest disturbances. BioScience 51 (9), 723–734.

Daly, C., Taylor, G.H., Gibson, W.P., 1997. The PRISM approach to mapping precipitation and temperature. In Proc., 10th AMS Conf. on Applied Climatology. pp. 20–23.

De Sales, F., Xue, Y., Okin, G.S., 2015. Impact of burned areas on the northern African seasonal climate from the perspective of regional modeling. Clim. Dynam., 1–21

Dore, S., Kolb, T.E., Montes-Helu, M., Eckert, S.E., Sullivan, B.W., Hungate, B.A., Kaye, J.P., Hart, S.C., Koch, G.W., Finkral, A., 2010. Carbon and water fluxes from ponderosa pine forests disturbed by wildfire and thinning. Ecol. Appl. 20 (3), 663–683.

Dore, S., Montes-Helu, M., Hart, S.C., Hungate, B.A., Koch, G.W., Moon, J.B., Finkral, A. J., Kolb, T.E., 2012. Recovery of ponderosa pine ecosystem carbon and water fluxes from thinning and stand-replacing fire. Glob. Change Biol. 18 (10), 3171–3185.

Ebel, B.A., 2013. Simulated unsaturated flow processes after wildfire and interactions with slope aspect. Water Resour. Res. 49 (12), 8090–8107.

Feikema, P.M., Sherwin, C.B., Lane, P.N., 2013. Influence of climate, fire severity and forest mortality on predictions of long term streamflow: potential effect of the 2009 wildfire on Melbourne's water supply catchments. J. Hydrol. 488, 1–16.

Keller, E.A., Valentine, D.W., Gibbs, D.R., 1997. Hydrological response of small watersheds following the Southern California Painted Cave Fire of June 1990. Hydrol. Process. 11 (4), 401–414.

Kinoshita, A.M., Hogue, T.S., 2011. Spatial and temporal controls on post-fire hydrologic recovery in Southern California watersheds. Catena 87 (2), 240–252.

Kinoshita, A.M., Hogue, T.S., 2015. Increased dry season water yield in burned watersheds in Southern California. Environ. Res. Lett. 10 (1), 014003.

LANDFIRE, 2010, Existing Vegetation Type Layer, LANDFIRE 1.2.0, U.S. Department of the Interior, Geological Survey. http://landfire.cr.usgs.gov/viewer/ (accessed 10.11.2017.).

LANDFIRE, 2012, Existing Vegetation Type Layer, LANDFIRE 1.3.0, U.S. Department of the Interior, Geological Survey. http://landfire.cr.usgs.gov/viewer/ (accessed 10.11.2017.).

LANDFIRE, 2014, Existing Vegetation Type Layer, LANDFIRE 1.4.0, U.S. Department of the Interior, Geological Survey. http://landfire.cr.usgs.gov/viewer/ (accessed 10.11.2017.).

LANDFIRE, LANDFIRE: Existing Vegetation Type, U.S. Department of Agriculture and U.S. Department of the Interior. https://www.landfire.gov/NationalProductDescriptions21.php. (accessed 10.11.2017.).
Lane, P.N., Sheridan, G.J., Noske, P.J., 2006. Changes in sediment loads and discharge from small mountain catchments following wildfire in south eastern Australia. J. Hydrol. 331 (3), 495–510.
Litvak, M., 2007a. AmeriFlux US-Vcm Valles Caldera Mixed Conifer, http://doi.org/10.17190/AMF/1246121.
Litvak, M., 2007b. AmeriFlux US-Vcp Valles Caldera Ponderosa Pine, http://dx.org/10.17190/AMF/1246122.
Liu, F., Bales, R.C., Conklin, M.H., Conrad, M.E., 2008. Streamflow generation from snowmelt in semi-arid, seasonally snow-covered, forested catchments, Valles Caldera, New Mexico. Water Resour. Res. 44 (12).
Micheletty, P.D., Kinoshita, A.M., Hogue, T.S., 2014. Application of MODIS snow cover products: wildfire impacts on snow and melt in the Sierra Nevada. Hydrol. Earth Syst. Sci. 18 (11), 4601.
Mitchell, P.J., Benyon, R.G., Lane, P.N., 2012. Responses of evapotranspiration at different topographic positions and catchment water balance following a pronounced drought in a mixed species eucalypt forest, Australia. J. Hydrol. 440, 62–74.
Monteith, J.L., 1965. Evaporation and environment. In Symp. Soc. Exp. Biol 19, 205–223, p. 4.
Montes-Helu, M.C., Kolb, T., Dore, S., Sullivan, B., Hart, S.C., Koch, G., Hungate, B.A., 2009. Persistent effects of fire-induced vegetation change on energy partitioning and evapotranspiration in ponderosa pine forests. Agri. For. Meteorol. 149 (3), 491–500.
Mu, Q., Zhao, M., Running, S.W., 2011. Improvements to a MODIS global terrestrial evapotranspiration algorithm. Rem. Sens. Environ. 115, 1781–1800.
Neary, D.G., Ryan, K.C., DeBano, L.F. 2005. Wildland fire in ecosystems: effects of fire on soils and water. General Technical Report RMRS-GTR-42-vol. 4. Ogden, UT: US Department of Agriculture, Forest Service, Rocky Mountain Research Station.
Nolan, R.H., Lane, P.N., Benyon, R.G., Bradstock, R.A., Mitchell, P.J., 2014. Changes in evapotranspiration following wildfire in resprouting eucalypt forests. Ecohydrology 7 (5), 1363–1377.
Nolan, R.H., Lane, P.N., Benyon, R.G., Bradstock, R.A., Mitchell, P.J., 2015. Trends in evapotranspiration and streamflow following wildfire in resprouting eucalypt forests. J. Hydrol. 524, 614–624.
PRISM Climate Group, Oregon State University, http://prism.oregonstate.edu, (created 4.02.2004.).
Remote Sensing Applications Center (RSAC). US. Forest Service. http://www.fs.fed.us/eng/rsac/baer/barc.html
Rollins, M.G., 2009. LANDFIRE: a nationally consistent vegetation, wildland fire, and fuel assessment. Int. J. Wildland Fire 18 (3), 235–249.
Parsons, A., Robichaud, P.R., Lewis, S.A., Napper, C., Clark, J.T., 2010. Field guide for mapping post-fire soil burn severity. Gen. Tech. Rep. RMRS-GTR-243. Fort Collins, CO: US Department of Agriculture, Forest Service, Rocky Mountain Research Station.
Sánchez, J.M., Bisquert, M., Rubio, E., Caselles, V., 2015. Impact of Land Cover Change Induced by a Fire Event on the Surface Energy Fluxes Derived from Remote Sensing. Rem. Sens. 7 (11), 14899–14915.
Savoca, M.E., Senay, G.B., Maupin, M.A., Kenny, J.F., Perry, C.A., 2013. Actual Evapotranspiration Modeling Using Operational Simplified Surface Energy Balance (SSEBop) Approach. US Geological Survey: Reston, VA, USA, pp.14
Senay, G.B., 2008. Modeling landscape evapotranspiration by integrating land surface phenology and a water balance algorithm. Algorithms 1 (2), 52–68.
Senay, G.B., Bohms, S., Singh, R.K., Gowda, P.H., Velpuri, N.M., Alemu, H., Verdin, J.P., 2013. Operational evapotranspiration mapping using remote sensing and weather datasets: a new parameterization for the SSEB approach. JAWRA J. Am. Water Resour. Assoc. 49 (3), 577–591.
Smith, H.G., Sheridan, G.J., Lane, P.N., Nyman, P., Haydon, S., 2011. Wildfire effects on water quality in forest catchments: a review with implications for water supply. J. Hydrol. 396 (1), 170–192.
Sun, G., McNulty, S.G., Amatya, D.M., Skaggs, R.W., Swift, L.W., Shepard, J.P., Riekerk, H., 2002. A comparison of the watershed hydrology of coastal forested wetlands and the mountainous uplands in the Southern US. J. Hydrol. 263 (1), 92–104.
Veenhuis, J.E., 2000. The effects of wildfire on the peak streamflow magnitude and frequency, Frijoles and Capulin Canyons, Bandelier National Monument, New Mexico. In Watershed Management and Operations Management 2000. pp. 1–3.
Velpuri, N.M., Senay, G.B., Singh, R.K., Bohms, S., Verdin, J.P., 2013. A comprehensive evaluation of two MODIS evapotranspiration products over the conterminous United States: Using point and gridded FLUXNET and water balance ET. Rem. Sens. Environ. 139, 35–49.
Vertessy, R.A., Watson, F.G., Sharon, K.O., 2001. Factors determining relations between stand age and catchment water balance in mountain ash forests. For. Ecol. Manage. 143 (1), 13–26.
Westerling, A.L., Hidalgo, H.G., Cayan, D.R., Swetnam, T.W., 2006. Warming and earlier spring increase western US forest wildfire activity. Science 313 (5789), 940–943.
Wine, M.L., Cadol, D., 2016. Hydrologic effects of large southwestern USA wildfires significantly increase regional water supply: fact or fiction? Environ. Res. Lett. 11 (8), 085006.
Yaseef, N.R., Yakir, D., Rotenberg, E., Schiller, G., Cohen, S., 2010. Ecohydrology of a semi-arid forest: partitioning among water balance components and its implications for predicted precipitation changes. Ecohydrology 3 (2), 143–154.
Zhou, Y., Zhang, Y., Vaze, J., Lane, P., Xu, S., 2013. Improving runoff estimates using remote sensing vegetation data for bushfire impacted catchments. Agricul. For. Meteorol. 182, 332–341.